Eur J Appl Physiol (1981) 46: 149–160

European Journal of
Applied
Physiology
and Occupational Physiology

Lactate After Exercise in Man: III. Properties of the Compartment Model

P. Zouloumian and H. Freund

Centre d'Etudes Bioclimatiques du CNRS,
21, rue Becquerel, F-67087 Strasbourg Cedex, France

Summary. Lactate movements during recovery following muscular exercise in man were studied by means of a two-compartment model. Mathematical discussion of the literal expressions obtained allows one to represent parameters concerning lactate exchange, utilization, and production in the previously working muscles and in the remaining lactate distribution space. It also shows that bi-exponential time courses predicted for muscular and blood lactate concentrations as well as for rates of lactate uptake, release, and utilization can denote several morphologies. All of the time evolutions for muscular and blood lactate concentrations found in the literature are consistent with these theoretical possibilities in the model. A numerical application confirms this concordance. Thus, this simple model, for which the basic assumptions were previously justified, appears to be qualitatively able to describe lactate exchanges and disappearance after exercise. A practical algorithm is put forward to display its possibilities and to test further its quantitative validity.

Key words: Two-compartment model properties – Time evolutions of lactate concentrations, fluxes

Introduction

Lactate movements for exercise recovery in man have been investigated theoretically by means of a two compartment model [13] for which the general solution expresses several correspondences among model parameters and time evolutions of lactate concentrations, rates of lactate production, uptake, release and utilization. The model could be tested through repeated numerical applications. But the present paper is designed to outline a general discussion of the model's properties by examination of the literal expressions obtained. When

Offprint requests to: Dr. P. Zouloumian (address see above)

0301-5548/81/0046/0149/$ 02.40

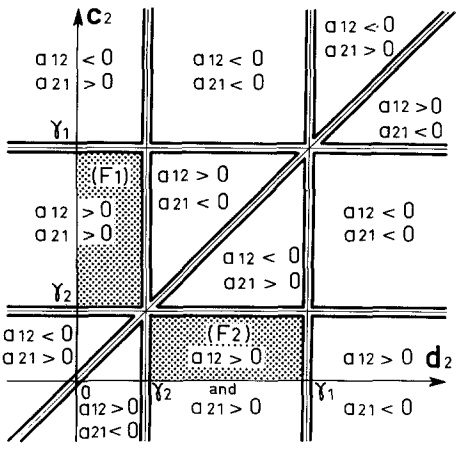

Fig. 1. Discussion of the signs of α_{12} and α_{21}; The domains (F_1) and (F_2) are the only ones for which the conditions $\alpha_{12} > 0$ and $\alpha_{21} > 0$ are conjointly satisfied

possible, the behaviors of the model will be qualitatively compared to experimental facts found in the literature. A graphical representation of the mathematical solution will be supplied.

Properties of the Model as They Appear Through the Literal Relationships

The assumptions (AS1), (AS2), (AS3), and (AS4) on which the model is based and the numbering of the relationships referred to in the present text are given in the previous paper [13]:

1. Scope of the Model

The predicted time functions of the model are defined for $t > 0$. The assumption (AS2) prescribes ($c_2 > 0$; $d_2 > 0$; $\alpha_{12} > 0$; $\alpha_{21} > 0$). Thus equations 35 and 36 delimit in the plane $(\overrightarrow{0\,d_2}, \overrightarrow{0\,c_2})$ two areas (F_1) and (F_2) in which the predictions of the model can be discussed. These areas correspond to ($\gamma_2 < c_2 < \gamma_1$; $0 < d_2 < \gamma_2$) and ($0 < c_2 < \gamma_2$; $\gamma_2 < d_2 < \gamma_1$), respectively[1] (Fig. 1). The conditions ($c_2 > d_2$) and ($c_2 < d_2$) attached respectively to (F_1) and (F_2) express the relative efficiencies of lactate utilization in (M) and (S).

2. The Predicted Parameters Within (F_1) and (F_2)

Relationship 32 defines in the plane $(\overrightarrow{0\,d_2}, \overrightarrow{0\,c_2})$ the general equation of conics (Γ) that depend on μ; these curves are real circles if $V_M \cdot L_M(\infty)$ equals $V_S \cdot L_S(\infty)$,

1 The cases of negative α_{12} and/or α_{21} [which violate (AS2)], that of $c_2 = d_2$, as well as those concerning the boundaries of (F_1) and (F_2) will not be discussed here

but become ellipses if not. The circles or ellipses contain the fixed points $\mathcal{M}_1$ (γ_1, γ_1) and $\mathcal{M}_2$ (γ_2, γ_2) and may intersect the coordinate axes. Moreover, their useful portions belong to (F_1) and (F_2). Relationship 33 gives two explicit definitions of (Γ): c_2 (+) and c_2 (−).

Likewise, the relations 35, 36, 38−41 as a function of d_2 show double definitions for α_{12}, α_{21}, $\mathcal{C}_1$, $\mathcal{C}_2$, $L_M(0)$ and c_1. Relationship 31 gives on the other hand a single definition for d_1. Applications can provide particular graphical depictions of these definitions (refer to Figs. 4 and 5).

3. *The Predicted Functions of Time*

According to equations 19 and 20, $L_M(t)$ and $L_S(t)$, as well as their linear combinations $[L_M(t) - L_S(t)]$, $\Phi_{mM}(t)$, $\Phi_{mS}(t)$, and $\Phi_{MS}(t)$, can be put in the form:

$$y(t) = y(\infty) - \alpha_1 \cdot e^{-\gamma_1 t} - \alpha_2 \cdot e^{-\gamma_2 t}, \quad (42)$$
(with $0 < \gamma_2 < \gamma_1$ and $t \geqslant 0$).

The properties of $y(t)$ can be summarized:

For $\alpha_2/\alpha_1 > 0$, its first two derivatives cannot become zero, and keep the same sign: hence, the so called "A-curves".

For $\alpha_2/\alpha_1 < 0$, its first two derivatives reduce to zero at the instants:

$$t_1 = (\gamma_1 - \gamma_2)^{-1} \cdot \log(-\gamma_1 \cdot \alpha_1/\gamma_2 \cdot \alpha_2) \quad (43)$$

and

$$t_2 = (\gamma_1 - \gamma_2)^{-1} \cdot \log\left(\frac{\gamma_1}{\gamma_2}\right) + t_1, \quad (44)$$

in which instance $y(t)$ shows an extremum followed by an inflexion point: hence, the so-called "B-curves".

The signs of t_1 and t_2 depend on the values of the coefficients. There results a large choice of graphs which have various senses of direction and boundaries. Thus, at $t \geqslant 0$, $L_M(t)$, $L_S(t)$, $[L_M(t) - L_S(t)]$, as well as $\Phi_{mM}(t)$, $\Phi_{mS}(t)$, $\Phi_{MS}(t)$ and their integrals can either:

(P1): preserve the same sign and reduce to zero one time at most

(P2): reduce once to zero before changing sign,

(P3): reduce to zero twice at most changing sign each time.

a) The Time Courses of $L_M(t)$ and $L_S(t)$:

The Predicted Morphologies: The discussion of the relationships 39 and 40 in (F_1) and (F_2) gives (Fig. 2):

$$(\mathcal{C}_1/\mathcal{D}_1 < 0;\ \mathcal{C}_2/\mathcal{D}_2 > 0)\,. \quad (45)$$

Thus, except in special cases enumerated in Footnote 1, if either $L_M(t)$ or $L_S(t)$ has an extremum and an inflexion point for $-\infty < t < +\infty$, the other does not: in spite of its apparent symmetry, the model predicts essentially different evolutions for the lactate concentrations in (M) and (S). Then for instance

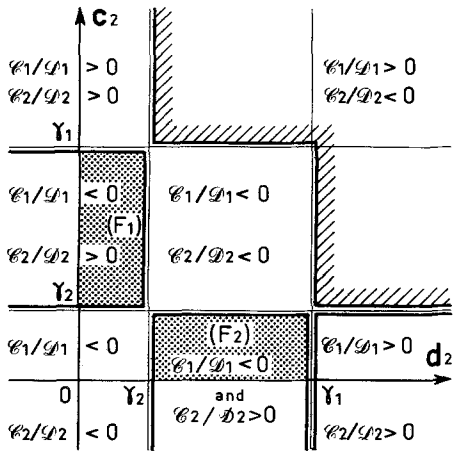

Fig. 2. The relations binding the coefficients of $L_M(t)$ and $L_S(t)$. The inequalities ($\mathscr{C}_1/\mathscr{D}_1 < 0$; $\mathscr{C}_2/\mathscr{D}_2 > 0$) occur in (F_1) and (F_2); thus, the pattern of $L_M(t)$ is not identical to that of $L_S(t)$

depiction of $L_M(t)$ with "A-curves" necessarily requires a description of $L_S(t)$ with "B-curves". More especially, decreasing $L_M(t)$ "A-curves" (i.e., with $\mathscr{C}_1 < 0$ and $\mathscr{C}_2 < 0$) leads the inequalities 45 to predict $\mathscr{D}_1 > 0$ and $\mathscr{D}_2 < 0$.

These predicted forms for the lactate concentration time courses agree qualitatively with the findings of several authors: Diamant et al. [3], Karlsson [9], Sahlin et al. [12], and Hermansen and Vaage [8] report the decreasing muscular "A-curves" that they observed during recovery. No muscular "B-curves" were given by these authors.

Among others, the investigations of Pernow et al. [11], Hermansen and Stensvold [6], Belcastro and Bonen [1], McGrail et al. [10], Bonen et al. [2], Hermansen et al. [7], Karlsson [9], and Sahlin et al. [12] show blood "B-curves" during recovery.

Other authors [4, 5] report accurate bi-exponential fits $L_a(t)$ which prove analytically that time courses of arterial lactate concentrations during recovery correspond to "B-curves". Using these results as well as the assumption (AS4) gives $\mathscr{D}_1 \simeq A_1 > 0$ and $\mathscr{D}_2 \simeq A_2 < 0$. This leads the model to predict decreasing muscular "A-curves" (with $\mathscr{C}_1 < 0$ and $\mathscr{C}_2 < 0$) which are qualitatively consistent with all the cited experimental observations.

The Relative Position of the Curves: The three behaviors (P_1), (P_2), or (P_3) for $[L_M(t) - L_S(t)]$ correspond to muscular and blood concentration curves without a common point, curves intersecting at one or two points, or tangent curves.

Experimental work reporting simultaneous muscular and blood lactate time evolutions during recovery are scarce. Diamant et al. [3], Hermansen and Vaage [8], as well as Karlsson [9] describe time courses of muscular and blood lactate concentrations that denote zero, one or two common points; tangent curves do not appear in these results.

b) The Time Courses of the Lactate Utilization Rates. According to (AS2) of reference [13], the predicted evolution curves of $\Phi_{mM}(t)$ and $\Phi_{mS}(t)$ are similar

to those of $L_M(t)$ and $L_S(t)$, respectively. The sum $[\Phi_{mM}(t) + \Phi_{mS}(t)]$ which estimates the instantaneous lactate utilization rate for the whole body also has a bi-exponential time evolution.

c) The Time Course of the Net Exchange Rate Between (M) and (S). Relationships 5, 29, 35, 36, 39, and 40 give:

$$\Phi_{MS}(t) = \mu - (\gamma_1 - d_2) \cdot V_S \cdot \mathscr{D}_1 \cdot e^{-\gamma_1 t} + (\gamma_2 - d_2) \cdot V_S \cdot \mathscr{D}_2 \cdot e^{-\gamma_2 t}. \quad (46)$$

The discussion of the coefficients $\alpha_1 = (\gamma_1 - d_2) \cdot V_S \cdot \mathscr{D}_1$ and $\alpha_2 = (\gamma_2 - d_2) \cdot V_S \cdot \mathscr{D}_2$ in this expression in (F_1) and (F_2) shows that $\Phi_{MS}(t)$ can reduce to zero none, one, or two times at the most, i.e., it denotes the properties (P_1), (P_2), or (P_3). Thus, it is an important consequence that according to equation 5, the arterial-venous lactate difference can become zero none, one or two times at the most, and the predicted net lactate exchange flow between (M) and (S) during recovery may be sometimes a net muscular release or a net muscular uptake.

More specifically, using (AS4) and the results reported elsewhere [4, 5] gives ($\mathscr{D}_1 > 0$; $\mathscr{D}_2 < 0$). Then (F_1), in which $d_2 < \gamma_2$, provides for $\Phi_{MS}(t)$ "B-curves" which can be consistent with graphs of observed $L_a(t)$ and $L_V(t)$ that denote either no common point, or tangency, or two common points. On the other hand, (F_2) in which $d_2 > \gamma_2$, supplies "A-curves": the corresponding evolutions of $L_a(t)$ and $L_V(t)$ may have a single common point without tangency.

All these theoretical possibilities are qualitatively consistent with the arterio-venous lactate differences observed by Pernow et al. [11] Hermansen et al. [7] and Hermansen and Vaage [8].

d) The Integrals of Lactate Fluxes. The time integrals of $\Phi_{mM}(t)$, $\Phi_{mS}(t)$, and $\Phi_{MS}(t)$ also have bi-exponential forms. These quantities give the amounts of lactate utilized in and exchanged between (M) and (S) and allow one to display the progress of recovery in the previously working muscles and in the whole body.

Representation of the Mathematical Solution

1. A Possible Strategy in Using the Formulae

Since the model expresses the relationships between several parameters and consequent time dependencies of lactate concentrations and flow rates, various choices of application are open to the user.

For instance, knowing $\Phi_{MS}(t)$ at the instants $t = \theta$, $t = \theta'$, and $t \to \infty$, equations 2 and 5 lead to the expressions:

$$d_2 = \frac{\Phi_{MS}(\theta) - \Phi_{MS}(\theta') - V_S\left[\left(\frac{dL_S}{dt}\right)_\theta - \left(\frac{dL_S}{dt}\right)_{\theta'}\right]}{V_S[L_S(\theta) - L_S(\theta')]}, \quad (47)$$

$$\mu = \Phi_{MS}(\theta) - V_S \cdot d_2\,[L_S(\theta) - L_S(\infty)] - V_S\left(\frac{dL_S}{dt}\right)_\theta, \quad (48)$$

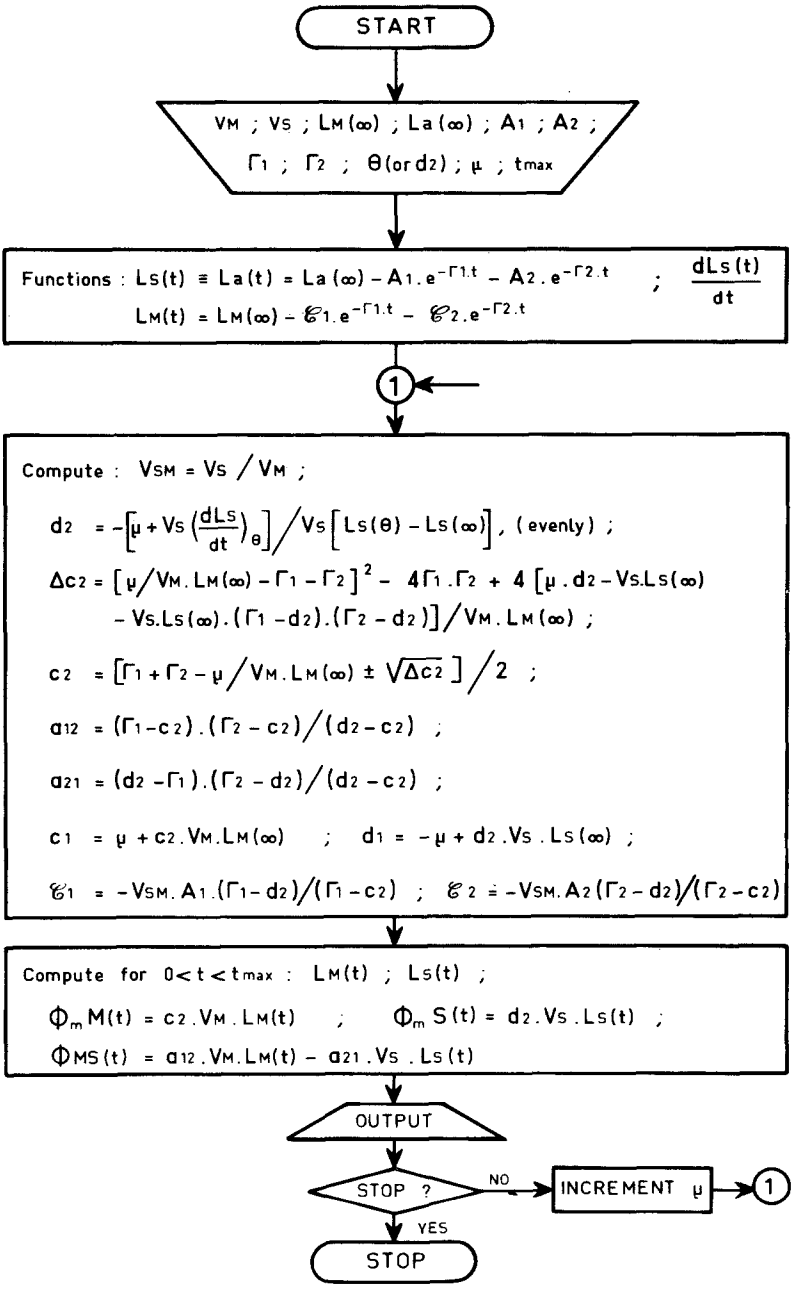

Fig. 3. A simple algorithm for calculations

which allow the computation of d_2 and μ in the general case if adequate information is supplied:

a) if θ and θ' correspond to the instants at which $[L_V(t) - L_a(t)]$ equals zero, d_2 and μ can be calculated from simplified relationships since $\Phi_{MS}(\theta) = \Phi_{MS}(\theta') = 0$;

b) if only one instant θ or θ' is known, d_2 can be calculated as a function of μ:

$$d_2 = -\frac{\mu + V_S\left(\frac{dL_S}{dt}\right)_\theta}{V_S[L_S(\theta) - L_S(\infty)]}. \tag{49}$$

According to (AS4) and using a numerical fit $L_a(t) = L_a(\infty) - A_1 \cdot e^{-\Gamma 1 \cdot t} - A_2 \cdot e^{-\Gamma 2 \cdot t}$ to observed arterial lactate concentrations, one can write the identities: $L_S(\infty) \equiv L_a(\infty)$; $\mathscr{D}_1 \equiv A_1$; $\mathscr{D}_2 \equiv A_2$; $\gamma_1 \equiv \Gamma_1$; $\gamma_2 \equiv \Gamma_2$. Thus the model predictions can be explored for given values of θ (or d_2), V_M, V_S, $L_M(\infty)$, and μ. Hence a practical algorithm for calculations (Fig. 3).

2. A Numerical Application

a) First Step. Using the algorithm and assuming $V_M = 20.24$ l; $V_S = 15.27$ l; $L_M(\infty) = L_S(\infty) = L_a(\infty) = 0.554$ mmol $\cdot$ l^{-1}; $\mathscr{D}_1 = A_1 = 9.18$ mmol $\cdot$ l^{-1}; $\mathscr{D}_2 = A_2 = -14.89$ mmol $\cdot$ l^{-1}; $\gamma_1 = \Gamma_1 = 0.509$ min^{-1}; $\gamma_2 = \Gamma_2 = 0.072$ min^{-1}, a numerical application of the model can be made for several values of the parameters μ and d_2; for instance:

-0.3 mmol $\cdot$ min$^{-1} \leqslant \mu \leqslant 0.3$ mmol $\cdot$ min^{-1} and $-\infty \leqslant d_2 \leqslant +\infty$.

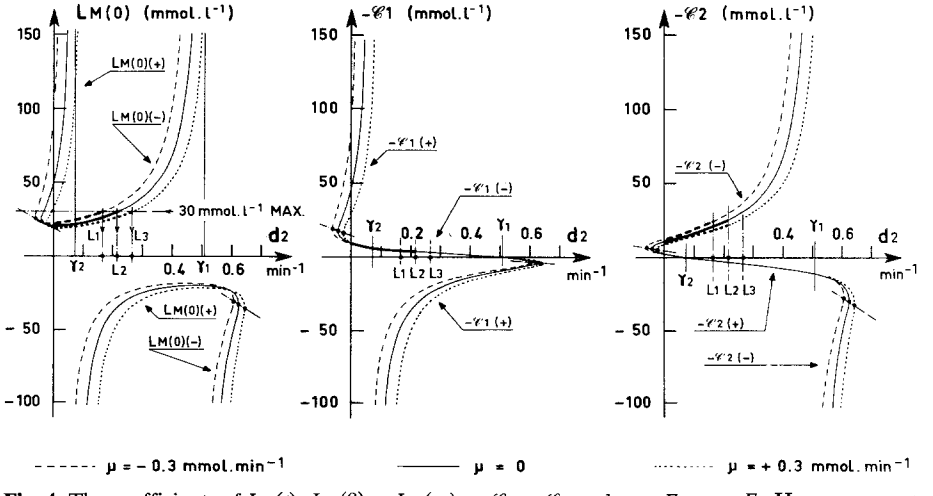

Fig. 4. The coefficients of $L_M(t)$: $L_M(0) = L_M(\infty) - \mathscr{C}_1 - \mathscr{C}_2$ and $\gamma_1 \equiv \Gamma_1$, $\gamma_2 \equiv \Gamma_2$. Heavy segments correspond to the useful portions of the curves

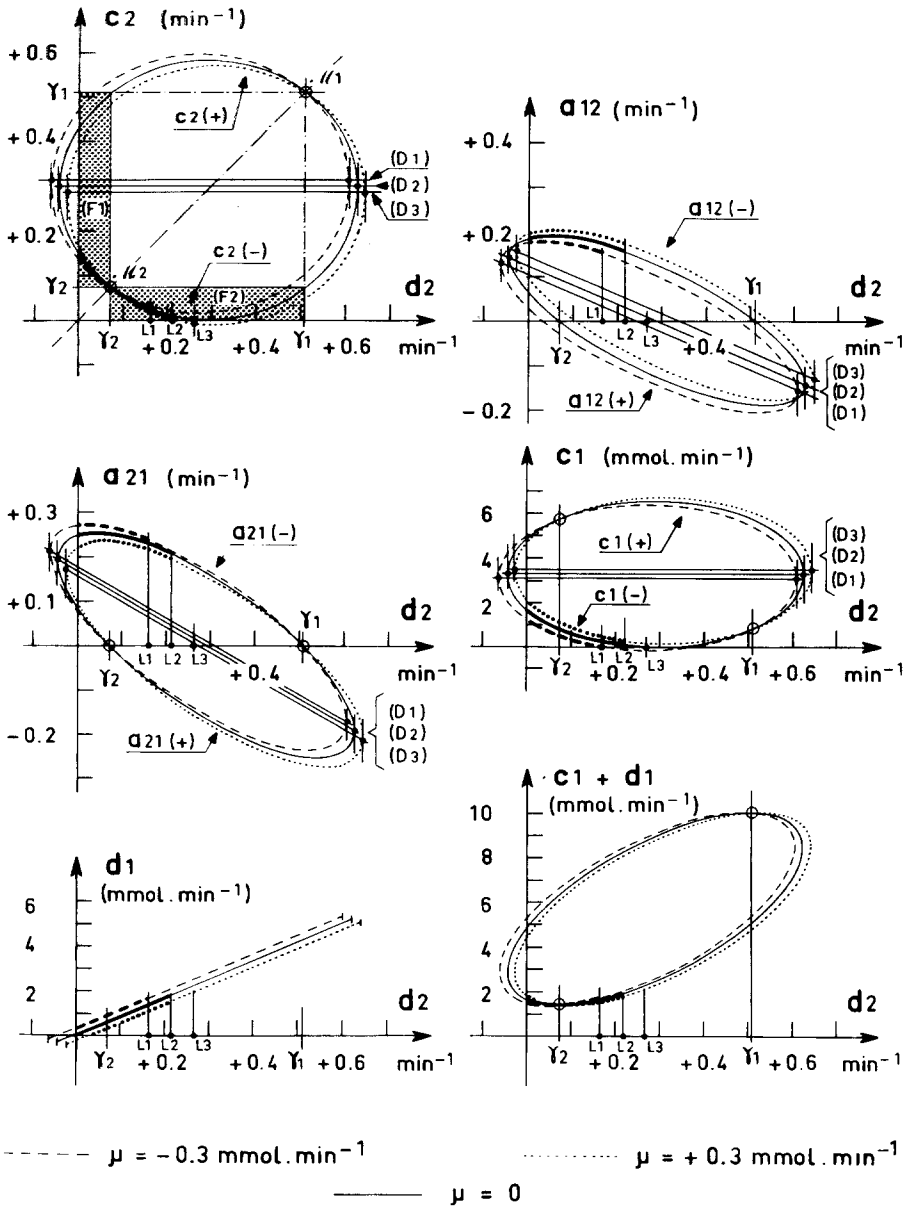

Fig. 5. The model's parameters. ($\gamma_1 \equiv \Gamma_1$ and $\gamma_2 \equiv \Gamma_2$)

Figure 4 represents as functions of d_2 and μ the coefficients $L_M(0)$, $-\mathscr{C}_1$ and $-\mathscr{C}_2$ of the function $L_M(t)$. Assuming a maximal value of 30 mmol $\cdot$ 1^{-1} for $L_M(0)$ shows that only the definition $L_M(0)$ $(-)$ is suitable here. Then:

the thresholds L_1, L_2, and L_3, which depend on μ, limit d_2; only the definitions "$(-)$" of the other parameters of the model can give realistic solutions.

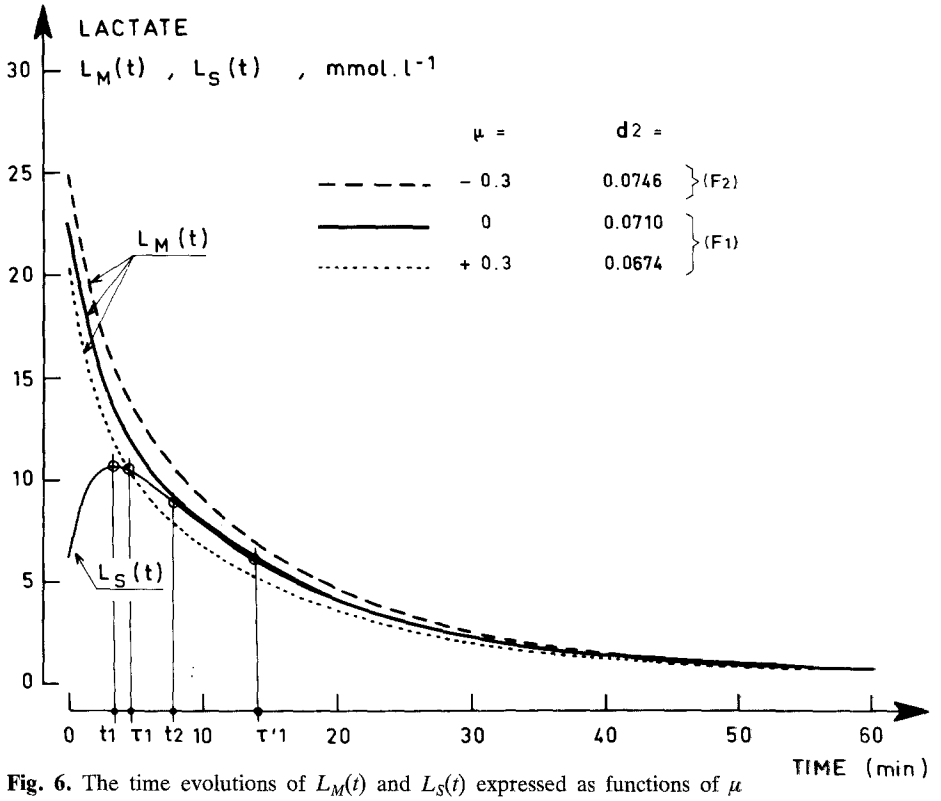

Fig. 6. The time evolutions of $L_M(t)$ and $L_S(t)$ expressed as functions of μ

In the present numerical case, the fulfilling of the inequality $c_2 > 0$ pushes the threshold L_3 not far from L_2 (see also Fig. 5).

Figure 5 represents the other parameters of the model as functions of d_2 and μ. The two definitions "(+)" and "(−)" of c_2, α_{12}, α_{21}, and c_1 appear on either side of the lines (D_1), (D_2), and (D_3), and the useful portions of the curves (heavy lines) result from the prescribed conditions $c_2 > 0$; $d_2 > 0$; $\alpha_{12} > 0$; $\alpha_{21} > 0$; $c_1 > 0$; $d_1 > 0$ as well as from the limitation of $L_M(0)$ to 30 mmol · l^{-1} (refer also to Fig. 4).

Notice that the useful portions of the ellipses (Γ) that describe the relation between c_2 and d_2 concern only a small part of the domains (F_1) and (F_2), and contain the fixed point $\mathcal{M}_2$.

If the values of μ and d_2 are known, a single numerical value can be assigned to each model parameter.

b) Second Step. Assuming $\theta = 14$ min, the value of d_2 can be computed for each μ. Fig. 6 represents the graphs of $L_M(t)$ and $L_S(t) \equiv L_a(t)$.

According to relationships 43 and 44, the function $L_S(t)$ attains its maximum at $t_1 \simeq 3.4$ min, and has a point of inflexion at $t_2 \simeq 7.9$ min.

For $\mu = +0.3$ mmol · min^{-1}, contact between the curves $L_M(t)$ and $L_S(t)$ takes place at $\tau_1 \simeq 4.6$ min; for $\mu = 0$, at $\tau'_1 \simeq 14$ min; and for $\mu = -0.3$

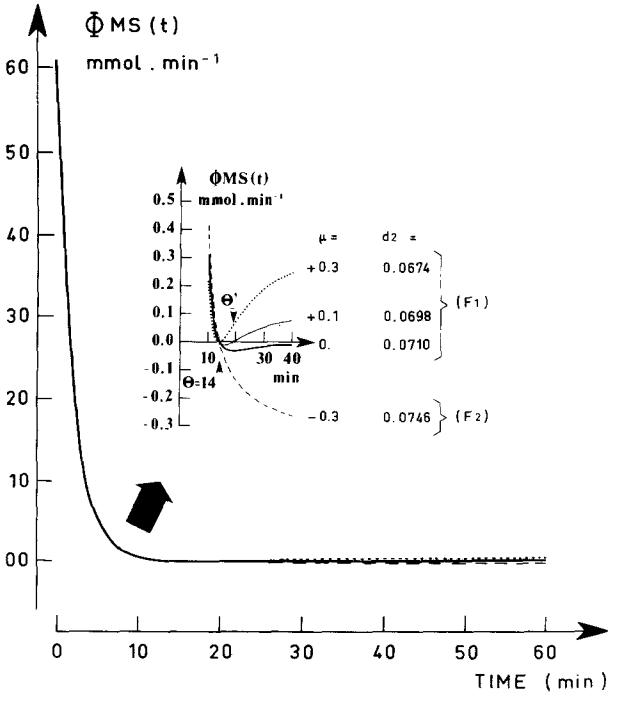

Fig. 7. The time evolutions of $\Phi_{MS}(t)$, as functions of μ

mmol · min^{-1}, at $t \to +\infty$. In the first two cases, which correspond to domain (F_1), the curve representing $L_M(t)$ crosses that of $L_S(t)$ and rejoins it for $t \to +\infty$. In the third case, which concerns domain (F_2) the $L_M(t)$ curve always lies above that of $L_S(t)$.

In other words, the time function $[L_M(t) - L_S(t)]$ can denote the properties (P_1) and (P_2).

According to relationships 3 and 4, the time courses of $\Phi_{mM}(t)$ and $\Phi_{mS}(t)$ show the same morphologies as those of $L_M(t)$ and $L_S(t)$, respectively.

Figure 7 illustrates the evolution of $\Phi_{MS}(t)$. Values of -0.3 mmol · min$^{-1} \leqslant \mu \leqslant 0.3$ mmol · min^{-1} give values of d_2 belonging either to (F_1) or (F_2); hence the predicted "A-curves" and "B-curves" that can denote any of the properties (P_1), (P_2), or (P_3).

For $\mu = 0.1$ mmol · min^{-1}, $\Phi_{MS}(t)$ becomes zero at a second instant $t = \theta'$.

Conclusion

The mathematical discussion of the literal expressions obtained shows several possible model behaviors concerning time evolutions for muscular and blood lactate concentrations, as well as for rates of lactate uptake, release, and utilization.

Since the simple two-compartment model was built on reasonable assumptions [13] its predictions were expected to be realistic. This appears to be the case; indeed, time courses of lactate concentrations in muscle and in arterial and venous blood as found in the literature are all at least qualitatively consistent with the theoretical possibilities of the model. The display of some model behaviors by means of a simple application to an experimental case confirms this agreement. Thus, the qualitative validity of the model in describing lactate movements during recovery following exercise can reasonably be considered to have been established. That the model can also supply acceptable quantitative predictions deserves to be examined through special experimental investigations.

List of Abbreviations and Symbols

α_{12}, α_{21}	Coefficients of efficiency in lactate transfer from (M) to (S) and (S) to (M), respectively (min^{-1})
A_1, A_2	Amplitudes of the exponential terms of fits to $L_a(t)$ (mmol · l^{-1})
(AS1), (AS2), (AS3), (AS4)	Assumptions on which the model is based
"A-curves"	Graphs of monotonic time functions
"B-curves"	Graphs of time functions showing an extremum and an inflexion point
c_1, d_1	Lactate production rates in (M) and (S), respectively (mmol · min^{-1})
c_2, d_2	Coefficients of efficiency in lactate utilization by (M) and (S), respectively (min^{-1})
$\mathscr{C}_1$, $\mathscr{C}_2$	Amplitudes of the exponential terms of $L_M(t)$ (mmol · l^{-1})
$\mathscr{D}_1$, $\mathscr{D}_2$	Amplitudes of the exponential terms of $L_S(t)$ (mmol · l^{-1})
(D_1), (D_2), (D_3)	Separating lines for definitions "(+)" and "(−)" of the parameters (Fig. 4)
(F_1), (F_2)	Areas of validity of the model
$L_a(t)$	Lactate concentration in arterial blood at time t obtained by fits to experimental data (mmol · l^{-1})
$L_M(t)$, $L_S(t)$	Lactate concentrations in (M) and (S), respectively, at time t (mmol · l^{-1})
$L_V(t)$	Lactate concentration in blood leaving (M) at time t (mmol · l^{-1})
L_1, L_2, L_3	Maximum allowable values for d_2 (Fig. 4) (min^{-1})
(M), (S)	Worked muscle space and remaining lactate space
$\mathscr{M}_1$, $\mathscr{M}_2$	Invariant points of (Γ)
(P_1), (P_2), (P_3)	Properties of the function $y(t)$
$q(t)$	Blood flow perfusing (M) at time t (l · min^{-1})
t	Time after the end of exercise (min)
t_1, t_2	Instants at which $y_t'(t)$ and $y_t''(t)$ reduce to zero (min)
V_M, V_S	Volumes of (M) and (S), respectively (l)
V_{MS}	V_M to V_S ratio
V_{SM}	V_S to V_M ratio
$y(t)$	General form of time functions generated by the model (mmol · l^{-1} or mmol · min^{-1})
α_1, α_2	Amplitudes of the transient terms of $y(t)$ (mmol · l^{-1} or mmol · min^{-1})
(Γ)	Conics describing the relation between c_2 and d_2
Γ_1, Γ_2	Velocity constants of the exponential fits to $L_a(t)$ (min^{-1})
γ_1, γ_2	Theoretical velocity constants of the time functions (min^{-1})
θ, θ'	Instants at which $\Phi_{MS}(t)$ reduces to zero (min)
μ	Net muscular release rate of lactate at $t \to \infty$ (mmol · min^{-1})
τ_1, τ_1'	Instants at which $L_M(t)$ crosses $L_S(t)$ (min)
$\Phi_{mM}(t)$, $\Phi_{mS}(t)$	Lactate utilization rates in (M) and (S), respectively (mmol · min^{-1})
$\Phi_{MS}(t)$	Net muscular release rate of lactate (mmol · min^{-1})

References

1. Belcastro AN, Bonen A (1975) Lactic acid removal rates during controlled and uncontrolled recovery exercise. J Appl Physiol 39: 932–936
2. Bonen A, Campbell CJ, Kirby RL, Belcastro AN (1979) A multiple regression model for blood lactate removal in man. Pflügers Arch 380: 205–210
3. Diamant B, Karlsson J, Saltin B (1968) Muscle tissue lactate after maximal exercise in man. Acta Physiol Scand 72: 383–384
4. Freund H, Gendry P (1978) Lactate kinetics after short strenuous exercise in man. Eur J Appl Physiol 39: 123–135
5. Freund H, Zouloumian P (1981) Lactate after exercise in man: I. Evolution kinetics in arterial blood. Eur J Appl Physiol 46: 121–133
6. Hermansen L, Stensvold I (1972) Production and removal of lactate during exercise in man. Acta Physiol Scand 86: 191–201
7. Hermansen L, Maehlum S, Pruett EDR, Vaage O, Waldum H, Wessel-Aas T (1975) Lactate removal at rest and during exercise. In: Howald H, Poortmans JR (eds). Metabolic adaptations to physical exercise. Birkhäuser, Basel, pp 101–105
8. Hermansen L, Vaage O (1977) Lactate disappearance and glycogen synthesis in human muscle after maximal exercise. Am J Physiol 233: E422–E429
9. Karlsson J (1971) Lactate and phosphagen concentrations in working muscle of man. Acta Physiol Scand 81: [Suppl] 358
10. Mc Grail JC, Bonen A, Belcastro AN (1978) Dependence of lactate removal on muscle metabolism in man. Eur J Appl Physiol 39: 89–97
11. Pernow B, Wahren J, Zetterquist S (1965) Studies on the peripheral circulation and metabolism in man. IV. Oxygen utilization and lactate formation in the legs of healthy young men during strenuous exercise. Acta Physiol Scand 64: 289–298
12. Sahlin K, Harris RC, Nylind B, Hultman E (1976) Lactate content and pH in muscle samples obtained after dynamic exercise. Pflügers Arch 367: 143–149
13. Zouloumian P, Freund H (1981) Lactate after exercise in man: II. Mathematical model. Eur J Appl Physiol 46: 135–147

Accepted January 3, 1981